

Chapter 1

Introduction

1.1 Background

The importance of surface acid/base properties in heterogeneous catalysis is apparent by the extensive amount of work dedicated to this topic [1-12]. Most of this work deals with oxide materials that have industrial applications like catalytic cracking and isomerization of hydrocarbons, alkylation of parafins and aromatics, polymerization of olefins, dehydration, dehydrogenation, and esterification [9,13]. Acid/base properties seem to be important in many organic reactions occurring over solid catalysts [6].

There is no general theory that serves as a basis for determining surface acidity and basicity [14]. Acidity and basicity depend on the nature of the oxide, the charge and radius of the metal ions, the character of the metal-oxygen bond as influenced by coordination numbers of the anions and cations, and the filling of the metal d-orbitals [14]. The Lewis acidity of low-coordination number transition metal cations and surface structural defects is not been well understood [15]. Well-defined single crystal oxide surfaces were used in this study to investigate directly the effect of cation coordination number on the strength of surface Lewis acid sites, and the effects of local site configuration and anion coordination number on CO_2 and BF_3 adsorption and its relationship to basicity. Three previously characterized metal oxide single crystals, $\text{Cu}_2\text{O}(111)$, $\text{SnO}_2(110)$ and $\text{Cr}_2\text{O}_3(10\bar{1}2)$, were investigated.

In the study of surface acid/base properties, the majority of work in the literature has been directed at understanding surface acidity, with much less effort directed at the study of surface basicity [16]. A variety of physicochemical techniques have been developed for the characterization of type, strength and numbers of acid sites on solid catalysts. One of the oldest techniques for measuring acidity is based on a proposal by Hammett [17] for ordering strengths of solid acids on the basis of amine titrations. Unfortunately, this method is strictly applicable only to protonic (Brønsted) acids. Since many oxide surfaces exhibit both protonic and aprotic (Lewis) acidity, both of which may interact with Hammett indicators, the nonspecificity of the indicator compromises the usefulness of the titration technique [6].

Acidity and basicity are characterized often in terms of the selectivities of probe reactions such as the dehydration/dehydrogenation of isopropanol [18]. Unfortunately, the presupposed reaction mechanisms on which these distinctions are made are greatly oversimplified [13]. For example, it has been shown that over ZnO [19,20], MgO [21] and TiO₂ [22,23] both dehydration and dehydrogenation of alcohols proceed through a common surface alkoxide intermediate. In these cases, the initial dissociative adsorption of the alcohols on acid or base sites is not what controls the product distribution, it is the selectivity between competing alkoxide decomposition channels. Hence, while the product distribution may be useful for characterizing materials as “acidic” or “basic”, the product molecules need not originate necessarily from different types of surface sites.

Other physicochemical techniques used to characterize surface acidity and basicity include the adsorption of acidic and basic gas phase probe molecules combined with spectroscopic measurements (IR) and calorimetric, gravimetric, or thermal desorption

measurements [1,2,4,6-11,14]. The use of these different techniques is closely related, and in combination can provide a characterization of type, number, and strength of acid/base sites on surfaces.

1.1.1 Surface Acidity

Two distinct types of surface acidity have been identified in the literature. Brønsted acidity is attributed to acidic protons on surface hydroxyl groups, while Lewis acidity is attributed to surface cations which can accept electronic charge from a donor (Lewis base) molecule [1-10]. These types of acidic sites are typically distinguished by infrared spectroscopic investigations of the adsorption of basic molecules (typically ammonia or pyridine) from the gas phase [1-10]. Mapes and Eischens [24] were the first to demonstrate the power and utility of IR studies of chemisorbed ammonia and provide direct experimental evidence for the existence of Lewis and Brønsted acidity on surfaces. Interactions of ammonia with strong Brønsted acid sites yields a surface ammonium cation, NH_4^+ , while interactions with Lewis acid sites give coordinated ammonia ($\text{NH}_3\cdot\text{L}$). Characteristic infrared modes for these species have been reported often [8,25-28]. Parry pioneered the similar use of pyridine as a probe molecule [29]. The 19b and 8a “ring” modes are most affected by intermolecular interactions with the nitrogen lone pair, and differences in these vibrational frequencies for hydrogen-bonded pyridine, coordinated pyridine (at Lewis acid sites), and pyridinium ion have been reported [8,10].

The use of ammonia or an amine as a probe molecule depends on the system of interest and the experimental conditions. Pyridine is sometimes preferred in cases where O-H stretching and H-O-H bending modes interfere with the IR identification of surface

species formed by ammonia adsorption [9]. Additionally, pyridine generally acts as a weaker base, and may be preferred where the properties of strongly acidic sites are to be probed (although this generalization cannot be applied universally) [6,8,10,29]. Other differences include the smaller molecular size of ammonia, and steric effects in the coordination of the different probe molecules to acidic sites. These properties can affect the number of different types of sites probed. Hence, while both molecules are used to probe similar surface properties, the details of the interactions can be dependent on the specific molecule and the specific surface investigated.

The two best methods for investigating the strength of acid sites appear to be calorimetric measurements of the heat of adsorption of base molecules and temperature programmed desorption (TPD) [6,10,11,14,30,31]. These techniques can provide a numeric measure of the strength of the chemisorption bond. Calorimetric measurements provide a quantitative thermodynamic scale of acidity by allowing a direct measure of the heat of adsorption of a probe molecule [11,31]. In particular, differential heats of adsorption can distinguish between sites of different strength, hence providing a measure of the number of energetically different sites as well as a thermodynamic measure of their acidity. Temperature programmed desorption also can provide a measure of the numbers of energetically different sites by the number of desorption features, the number density of each type of site by the intensity of the desorption features, and the strength of the sites based on the desorption temperatures of the probe molecule. The TPD method is simple, rapid, and reproducible [30,32], and can provide a quantitative determination of the activation energies of desorption. While problems are encountered in the determination of activation energies of desorption of powders [11,33-36], they are straightforward to

evaluate from TPD measurements of low-surface area single crystal samples in ultrahigh vacuum. A variety of methods exist for the determination of desorption kinetics parameters [37].

1.1.2 Surface Basicity

Brønsted acids have been used as probe molecules for surface basicity, but organic acids are of sufficient strength that they generally react with even weakly basic surfaces. Weaker Brønsted acids such as water, alcohols, alkenes, and alkynes can be used [38], but they do not react simply with basic sites, they react with acid/base site pairs. This principle is clearly illustrated by work on the adsorption of Brønsted acids on the polar ZnO (0001) surfaces by Vohs and Barteau [39,40]. The dissociation of Brønsted acids (even strong organic acids) is only observed on surfaces exposing acid/base site pairs. The large anions on the (0001)-O surface obscure the second atomic layer cations and make them inaccessible to the adsorbate, hence no dissociation occurs. Conversely, the zinc cations in the outer atomic layer of the (0001)-Zn surface are small, and the large second-layer oxygen anions are accessible to the adsorbate (cation/anion pairs are available) and dissociation occurs [40-42].

Little is known about the surface properties of oxides that lead to basicity. Surface base sites are typically considered to be electron rich surface oxygen anions, which can donate electronic charge or bind acidic protons to form surface hydroxyl groups [1,43]. Attempts to study surface basicity typically employ acidic probe molecules. The probe molecule most often employed is CO₂ [10,11,14], which can poison reactions thought to proceed over basic surface sites [10].

The most common types of surface species reported from CO₂ adsorption on oxides are carbonates and bicarbonates. The adsorption of CO₂ to form a carbonate anion (CO₃⁻²) can be viewed simplistically as the insertion of a basic surface oxygen anion into CO₂, while the formation of bicarbonate (HCO₃⁻) might be viewed as the insertion of a surface “Brønsted base” site. While there is little mention in the literature of surface “Brønsted base” sites, the hydrogen bonding of ammonia to non-acidic surface hydroxyl groups is mentioned often. In fact, the interaction of CO₂ with oxide surfaces is far more complex. Both monodentate and bidentate surface carbonates have been identified by IR over a number of different metal oxides [7,10]. For example, one monodentate carbonate and two energetically different bidentate carbonates have been observed over Cr₂O₃ powder surfaces. The formation of the weaker bidentate carbonate and the monodentate carbonate are believed to occur at cation sites with one coordination vacancy, while the stronger bidentate carbonates are postulated to involve surface cations initially with two coordination vacancies [10,44]. Likewise, the formation of surface bicarbonate species requires coordinately unsaturated cations on partially hydroxylated Cr₂O₃ surfaces [10,44]. Similar suggestions regarding the role of coordinately unsaturated cations in CO₂ adsorption have been made regarding alumina and magnesia surfaces [10].

The infrared identification of carbonates, bicarbonates, carboxylates and perturbed CO₂ molecules has been reviewed by Busca and Lorenzelli [7]. Surface carbonate species are generally identified by the appearance of ν_3 (asymmetric CO stretch) bands in the vicinity of 1400 cm⁻¹. Lower frequency modes are also present, but their use is often complicated by overlapping with the metal-oxygen stretching bands of the oxides themselves. Identification of the coordination of the carbonate species is usually made on

the basis of the splitting of the degenerate ν_s modes [7]. Surface bicarbonate species can be identified by modes at 3150-3340 cm^{-1} (νOH), 1670-1700 cm^{-1} (asymmetric $\nu\text{C=O}$), 1320-1350 cm^{-1} (symmetric $\nu\text{C=O}$) and 1200-1252 cm^{-1} (νOH) [7]. These values can be modified somewhat by hydrogen bonding interactions [7].

Another possible probe molecule for Lewis basicity is boron trifluoride (BF_3). BF_3 is a planar, monomeric, strong Lewis acid [45]. It is a stable gas as BF_3 and does not dimerize like BH_3 [45]. The boron atom of BF_3 has only six electrons in its outer shell and has a tendency to combine with atoms having unshared electron pairs to form a stable electronic configuration of eight electrons in the outer shell [45]. The boron atom of BF_3 has one empty p_z -orbital which is perpendicular to the plane of the molecule [45]. BF_3 is a typical Lewis acid where the empty orbital of the boron atom has a tendency to accept an electron pair [45]. BF_3 forms bonds that are covalent in nature due to the strong bonding interaction with the lone pair electrons from the donor atoms [45]. Upon bonding to a donor, the boron increases its coordination number from three to four, which likely involves a change in configuration of BF_3 from planar to tetrahedral [45]. Oxygen is one known atom that has been found to donate electrons to the boron atom of BF_3 [45]. Therefore, BF_3 was studied to investigate the possibility that it can selectively interact with surface Lewis base sites such as oxygen anions in metal oxides.

1.2 Surfaces Investigated

For many years, acid/base characterizations have been used to explain catalytic chemistry without using well-defined surfaces. There have been very few descriptions of acid/base properties of specific surface sites on metal oxides with known coordination

numbers and oxidation states. The well-defined, single crystal surfaces of Cu_2O , SnO_2 and Cr_2O_3 have been investigated with this in mind.

Cu_2O and SnO_2 show interesting behavior in acid/base reactions for the dissociation of weak Brønsted acids. In both cases, specific oxygen vacancies on each surface have been found to catalyze the dissociation reactions of particular molecules. The more ideal surfaces do not dissociate weak Brønsted acids under UHV conditions. Therefore, the ability of the surface to promote a dissociation reaction depends on the preparation and condition of the surface. In previous studies involving polar ZnO (0001), lack of reactivity on the O-terminated polar surface was due to the absence of accessible cation/anion pairs that were necessary for dissociative adsorption [39]. Cu_2O and SnO_2 surfaces have cation/anion pairs that are always available, hence changes in behavior cannot be related to the accessibility. Therefore, the specific surface features on these surfaces are required to promote the dissociation reaction.

1.2.1 Cu_2O (111)

The non-polar Cu_2O (111) single crystal surface has been characterized previously [46]. The non-polar Cu_2O (111) surface can be prepared in a stoichiometric form (Figure 1.1 (a)) or a non-stoichiometric form (Figure 1.1 (b)) that is associated with a loss of one-third of the outer-layer of oxygen anions. The oxygen anions in the outer atomic layer have a coordination of three on the (111) surfaces. The bulk coordination of the Cu^+

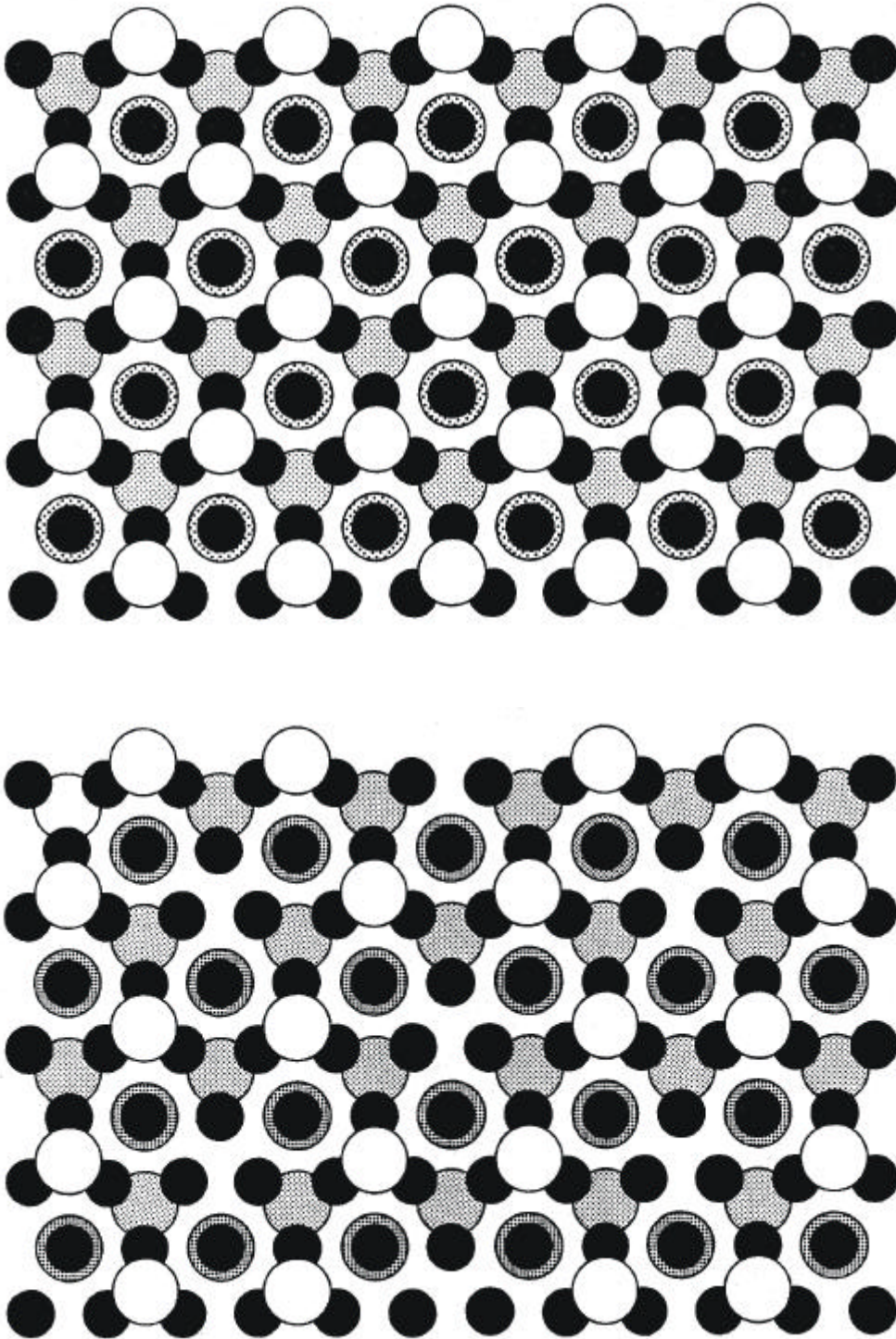


Figure 1.1 Ball model illustrations of Cu_2O (111): (a) the ideal, stoichiometric surface, (b) the $(\sqrt{3} \times \sqrt{3})R30^\circ$ surface with one-third oxygen vacancies. The small solid circles represent Cu cations while the large open circles represent O^{2-} anions. Increased shading of the oxygen anions represents increased depth away from the surface. The illustrations assume no relaxation.

cation is two, and the exposed surface cations are singly coordinate. Using these two surfaces, the adsorption behavior on sites associated with anion vacancies can be tested with no change in the coordination of the surface cations, just changes in local geometry.

The adsorption and dissociation of propene at low temperatures (100 K) and low pressure ($<10^{-6}$ Torr) has been investigated previously on these surfaces [46]. Since the methyl hydrogens are the most acidic for gas phase propene, the dissociation to allyl can be viewed in acid/base terms as the dissociation of a weak Brønsted acid to a proton and an allyl anion. Only the oxygen deficient, $(\sqrt{3}\times\sqrt{3})R30^\circ$ Cu_2O (111) surface (Figure 1.1 (b)) has been found to activate the dissociative acid/base reaction of propene to surface allyl at low temperature. In previous TPD experiments, the recombination of surface allyl and hydrogen for propene desorption has been clearly associated with the presence of the oxygen vacancies on this surface [46,61]. The Lewis acidity of these sites has been implicated in their ability to dissociate a weak Brønsted acid.

1.2.2 SnO_2 (110)

SnO_2 surfaces have been characterized in previous work [47-49]. Different surface compositions can be prepared by ion bombardment and oxidation/reduction treatments. The ideal, stoichiometric surface is prepared by exposure to nitrous oxide at high temperature and pressure and consists of an outer layer of coordinately unsaturated oxygen anions with an exposed second layer consisting of five-coordinate Sn^{4+} cations and three-coordinated oxygen anions (Figure 1.2 (a)). The "reduced" surface is obtained

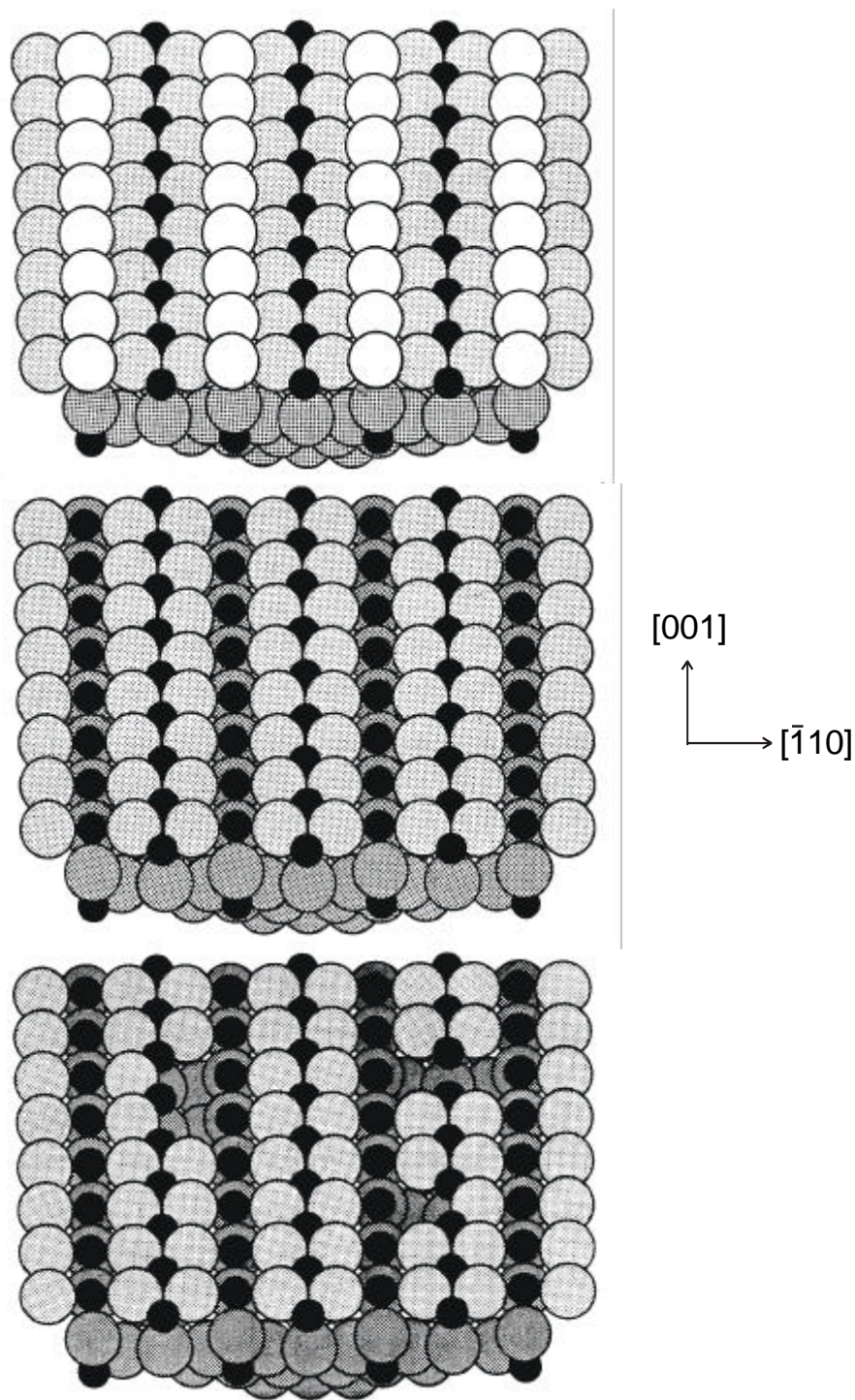


Figure 1.2 Ball model illustrations of SnO₂ (110): (a) the ideal, stoichiometric surface, (b) the “reduced” surface missing all bridging oxygen anions and (c) the “defective” surface with the in-plane oxygen vacancies. The small solid circles represent Sn cations while the large open circles represent O²⁻ anions. Increased shading of the oxygen anions represents increased depth away from the surface. The illustrations assume no relaxation.

by heating the stoichiometric surface to 700 K and removing the outer bridging oxygen anions exposing four-coordinate Sn^{2+} cations to the surface (Figure 1.2 (b)). Heating the stoichiometric surface to 1000 K creates a defective surface that has some in-plane oxygen anions removed creating sites that have a cation coordination number of three associated with these point defects (Figure 1.2 (c)). A “less-defective” surface prepared by oxidation followed by annealing to 1000 K has an estimated 20% in-plane oxygen vacancies, while a “highly-defective” surface created by Ar^+ ion bombardment and annealing to 1000 K has an estimated 50% in-plane oxygen vacancies [50].

Methanol shows some interesting behavior on SnO_2 (110). Methanol is adsorbed molecularly on the stoichiometric SnO_2 (110) surface. Methanol dissociates to a proton and a methoxide anion on the "reduced" SnO_2 (110) surface. As in-plane oxygen vacancies are created, the dissociation of methanol shuts down and the surface adsorbs methanol molecularly. Therefore, the most stoichiometric and most oxygen-deficient surfaces have the least activity for methanol dissociation. Methanol dissociation is thought to be dependent primarily on the properties of the surface cations [51].

1.2.3 Cr_2O_3 ($10\bar{1}2$)

$\alpha\text{-Cr}_2\text{O}_3$ is an electrical insulator (band gap = 3.4 eV) with the corundum structure [52,53]. The bulk chromium coordination geometry is a distorted octahedron, and oxygen anions are coordinated by a distorted tetrahedral arrangement of cations. In the corundum structure, one third of the possible cation sites are vacant. These vacancies are located along the ($10\bar{1}2$) and other crystallographically equivalent planes [54].

The Cr_2O_3 ($10\bar{1}2$) surface has been characterized in previous work [55]. The ideal, stoichiometric surface has only one local coordination environment for the surface cations and anions. A ball model representation of the ideal, stoichiometric surface is shown in Figure 1.3. The topmost atomic layer of the ideal surface is composed entirely of oxygen anions. One full stoichiometric repeating unit normal to the surface contains five atomic layers arranged as [O, Cr, O, Cr, O]. The surface has a rectangular (almost square) periodicity with a ratio of sides of $a/b = 0.94$. At the ($10\bar{1}2$) surface, all O^{2-} anions in the top atomic layer are three-coordinate with a pyramidal local coordination, and the Cr^{3+} cations contained in the second atomic layer are five-coordinate. Both ions have one degree of coordinate unsaturation relative to their bulk counterparts [56]. All ions below the top two atomic layers are fully-coordinated. The nearly-stoichiometric surface was prepared by sputtering the surface with Ar^+ ions and annealing the surface at 900 K for five minutes [55].

Surface cations on the stoichiometric surface may be capped with terminal chromyl oxygen ($\text{Cr}=\text{O}$) or Cl adatoms. An oxygen-terminated surface can be prepared by successive low temperature oxygen exposures on a nearly-stoichiometric surface until nearly all surface cations are saturated with oxygen [55]. The oxygen-terminated surface exposes both the three-coordinate O^{2-} anions and the chromyl oxygen anions ($\text{Cr}=\text{O}$) [55].

A chlorine-terminated surface can be prepared by successive low temperature 1,1,2 trichloro-1 fluoroethane exposures on a nearly-stoichiometric surface. 1,1,2-trichloro-fluoroethane decomposes primarily into $\text{CFCl}=\text{CH}_2(\text{g})$, and adsorbed chlorine [57]. The dihaloelimination reaction can be thought of as the oxidation of a vicinal

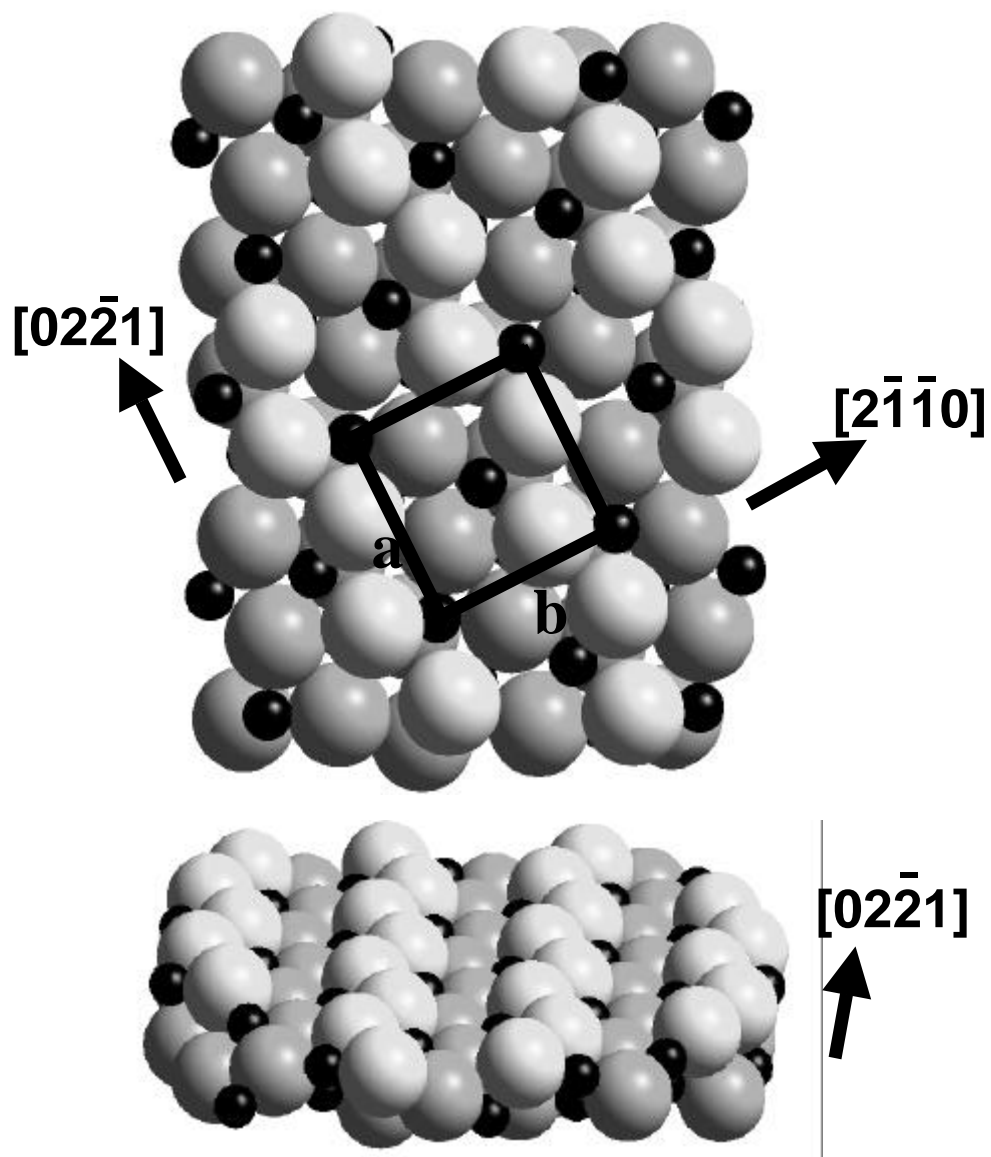


Figure 1.3 A ball model representation of the Cr_2O_3 $(10\bar{1}2)$ surface. The top view shows the $(10\bar{1}2)$ surface parallel to the plane of the page. A surface unit cell is drawn to show the periodicity. The bottom shows a side view of one stoichiometric repeating layer. The chromium cations are represented by small black spheres and oxygen anions by the large gray spheres.

dihalide to an alkene. The decomposition of $\text{CFCl}_2\text{CH}_2\text{Cl}$ results in a significant build-up of chlorine on the sample surface where an estimated one chlorine atom is adsorbed for every five-coordinate chromium atom exposed at the surface [57]. The chlorine-terminated surface exposes three-coordinate O^{2-} anions and Cl adatoms.

1.3 Experimental

All single crystal samples were separately mounted on a tantalum holder, which acted as an indirect heating and cooling source and provided mechanical stability. The holder was supported by two 1 mm tantalum wires connected to LN_2 -cooled copper electrical feed-throughs in a sample rod manipulator. The sample temperature was monitored using a type-K thermocouple bonded directly to the back of the crystal with Aremco No. 569 ceramic cement. Hence, direct measurements of the crystal temperature were possible.

The Cu_2O crystal used for this study was grown by a float zone technique using an arc image furnace [58]. The crystal was aligned using Laue back-reflection, and mechanically polished to within 0.5° of the (111) surface [46]. Sample dimensions were approximately $7 \times 5 \times 1 \text{ mm}^3$. The SnO_2 crystal used in this study was grown by the vapor-phase transport method of Thiel and Helbig [59], oriented by Laue back reflection, and mechanically polished to within 1° of the (110) surface [47-49]. The dimensions of the sample are approximately $4 \times 3 \times 1/2 \text{ mm}^3$. The Cr_2O_3 crystal was oriented to within 1° of the $(10\bar{1}2)$ surface using Laue back-reflection and polished to a final mirror finish with $0.25 \mu\text{m}$ diamond paste [55].

Experiments were conducted in two different ultrahigh vacuum (UHV) systems. One system is a turbo-pumped, dual-chamber vacuum system equipped with a Leybold EA-11 hemispherical analyzer, a dual Mg/Al anode X-ray source for X-ray photoelectron spectroscopy (XPS), and a differentially-pumped DC discharge lamp for ultraviolet photoelectron spectroscopy (UPS). The ultraviolet light had an incident angle of 55° with respect to the surface normal. The UPS data were collected with an analyzer resolution (ΔE) of 0.15 eV. The binding energies were referenced to the Fermi level, determined from the tantalum holder in contact with the sample. The second system is an ion-pumped, Physical Electronics chamber, equipped with a Model 15-155 single-pass CMA for Auger electron spectroscopy (AES). Both systems also include an Inficon Quadrex 200 mass spectrometer for thermal desorption spectroscopy (TDS) and a set of Vacuum Generators three-grid, reverse-view, low-energy electron diffraction (LEED) optics.

Gas exposures were performed by backfilling the chamber through a variable leak valve. Matheson research grade NH_3 (99.995%) was used as received. The CO_2 used was from AIRCO Gases, grade 5.5 SFC, having less than 5 PPM impurities. The BF_3 used was from Aldrich, having a purity of 99.5%. A 2 K/sec heating rate was used for all TDS experiments. The low heating rate was used to minimize the possibility of thermally fracturing the ceramic samples. The mass spectrometer was equipped with a glass skimmer to minimize the sampling of desorption products from the crystal support hardware. All doses were corrected for ion gauge sensitivity except for BF_3 exposures [60]. During TDS experiments, the background pressure was less than 2×10^{-10} Torr between doses.

Oxidation treatments of the SnO₂ (110) surface were performed using Matheson SCF grade N₂O (99.995%) at 1.0 Torr. The sample was heated to 700 K at a rate of 2 K/sec, held for 2 minutes, and cooled to 310 K before the chamber was evacuated of N₂O. After the chamber pressure decreased to 2×10⁻⁹ Torr, the cryopanel was exposed to LN₂ to reduce the pressure to 3×10⁻¹⁰ Torr. To reduce the pressure into the low to mid 10⁻¹⁰ Torr range within a reasonable amount of time, only one oxidation treatment was run per day.

A nearly-stoichiometric Cu₂O (111) surface is prepared by argon ion bombardment and annealing to 1000 K in vacuum resulting in a (1×1) LEED periodicity (Figure 1.1 (a)) [46]. A (√3×√3)R30° Cu₂O (111) surface is prepared by repeated 200 L exposures of H₂ with a red hot filament to crack the H₂ (Figure 1.1 (b)) [46]. Such treatments lead to the removal of an ordered one-third of a layer of oxygen resulting in a (√3×√3)R30° LEED periodicity [46]. Each oxygen vacancy gives rise to a threefold site of singly-coordinate Cu⁺ cations. LEED and propene adsorption are used to check the surface condition. Using a 0.06 L exposure of propene, a (√3×√3)R30° surface is identified in TDS by an increased intensity in the 330 K desorption feature and decreased intensity in the 240 K feature [61].

Oxidation treatments of Cr₂O₃ (10 $\bar{1}$ 2) were performed using Matheson SCF grade O₂ (99.995%) as received. Successive 0.13 L exposures at 190 K followed by heating to 700 K were performed to obtain an oxygen-terminated surface [55]. Chlorination treatments of Cr₂O₃ (10 $\bar{1}$ 2) were performed using PCR 1,1,2-trichloro-1-fluoroethane (97%) as received. Successive 0.13 L exposures of 1,1,2-trichloro-1-fluoroethane

(CFCl₂CH₂Cl) at 190 K with heating to 700 K were used to create a chlorine-terminated surface [57].

1.4 Overview of Work

The objective of this work is to study the interaction of acid/base probe molecules with specific sites on well-defined oxide surfaces. The Lewis acidity and basicity of these specific sites on well-defined surfaces of Cu₂O, SnO₂, and Cr₂O₃ were characterized using probe molecules to give insight to their chemistry. Where possible, the relationship between the Lewis acidity and basicity of these specific sites and their ability to dissociate a weak Brønsted acid has been discussed. These specific sites on the well-defined surfaces were used to examine the effect of changes in local geometry of cation types on the Lewis acidity and the effect of changes in local geometry of cation/anion pairs on the Lewis basicity. NH₃ was used as the basic probe molecule for interrogating acid sites, and CO₂ and BF₃ were tested for their ability to provide a characteristic measure of the basicity of specific surface features.

1.5 References

-
- [1] K. Tanabe, **Solid Acids and Bases** (Academic Press, New York, 1970).
- [2] K. Tanabe, M. Misono, Y. Ono, and H. Hattori, **New Solid Acids and Bases** (Elsevier, Amsterdam, 1989.)
- [3] D. Barthomeuf in **Catalysis by Acids and Bases**, Ed. B. Imelik, C. Naccache, G. Coudurier, Y. Ben Taarit and J. C. Vedrine (Elsevier, Amsterdam, 1985) p.75.
- [4] K. Tanabe in **Catalysis: Science and Technology**, Vol.2, Ed. J.R. Anderson and M. Boudart (Springer-Verlag, Berlin 1981) p.231.
- [5] J.P. Bohm and Knozinger in **Catalysis: Science and Technology**, Vol.4, Ed. J.R. Anderson and M. Boudart (Springer-Verlag, Berlin 1981) p.367.
- [6] J. Kijenski and A. Baiker, *Catal. Today*, **5** (1989) 1.
- [7] G. Busca and V. Lorenzelli, *Materials Chemistry*, **7** (1982) 89.
- [8] M.C. Kung and H.H. Kung, *Catal. Rev.-Sci. Eng.*, **27** (1985) 425.
- [9] H.A. Benesi and B.H.C. Winquist, *Adv. Catal.*, **27** (1978) 97.
- [10] H. Knozinger, *Adv. Catal.*, **25** (1976) 184.
- [11] N. Cardona-Martinez and J.A. Dumesic, *Adv. Catal.*, **38** (1992) 149.
- [12] M.S. Goldstein in **Experimental Methods in Catalytic Research**, Ed. R.B. Anderson (Academic Press, New York, 1968) p.361.
- [13] R.N. Spitz, J.E. Barton, M.A. Barteau, R.H. Staley and A.W. Sleight, *J. Phys. Chem.*, **90** (1986) 4067.
- [14] A. Auroux and A. Gervasini, *J. Phys. Chem.*, **94** (1990) 6371.
- [15] Z.M. Zhidomirov and V.B. Kazansky, *Adv. Catal.*, **34** (1986) 131.
- [16] P.F. Rossi, G. Busca, V. Lorenzelli, M. Lion and J.C. Lavalley, *J. Catal.*, **109** (1988) 378.
- [17] L.P. Hammett, *Chem. Rev.*, **16** (1935) 67.
- [18] M. Ai, *Bull. Chem. Soc. Jpn*, **50** (1977) 2579.
- [19] M. Bowker, E. Houghton, K.C. Waugh, *J. Chem. Soc., Faraday Trans. 1*, **78** (1982) 2573.
- [20] J.M. Vohs and M.A. Barteau, *J. Chem. Phys.*, **95** (1991) 297.
- [21] S.L. Parrott, J.W. Rogers Jr. and J.M. White, *Appl. Surf. Sci.*, **1** (1978) 443.
- [22] K.S. Kim and M.A. Barteau, *J. Mol. Catal.*, **63** (1990) 103.
- [23] K.S. Kim, M.A. Barteau and W.E. Farneth, *Langmuir*, **4** (1988) 533.
- [24] J.E. Mapes and R.P. Eischens, *J. Phys. Chem.*, **58** (1954) 1059.
- [25] A.A. Tsyganenko, D.V. Pozdnayakov and V.N. Filimonov, *J. Mol. Struct.*, **29** (1975) 299.
- [26] K. Morishige, S. Kittaka, S. Katsuragi and T. Morimoto, *J. Chem. Soc., Faraday Trans 1*, **78** (1982) 2947.
- [27] T. Morimoto, H. Yanai and M. Nagao, *J. Phys. Chem.*, **80** (1976) 471.
- [28] L.H. Little, **Infrared Spectra of Adsorbed Species**, Academic Press, New York, 1966.
- [29] E.P. Parry, *J. Catal.*, **2** (1963) 371.
- [30] P. Berteau and B. Delmon, *Catal. Today*, **5** (1989) 121.
- [31] N. Cardona-Martinez and J.A. Dumesic, *J. Catal.*, **128** (1991) 23.

-
- [32] P.A. Redhead, *Vacuum*, **12** (1962) 203.
- [33] J.A. Konvalinka, J.J.F. Scholten and J.C. Rasser, *J. Catal.*, **48** (1977) 365.
- [34] E.E. Ibok and D.F. Ollis, *J. Catal.*, **66** (1980) 391.
- [35] D.M. Jones and G.L. Griffin, *J. Catal.*, **80** (1983) 40.
- [36] J.S. Rieck and A.T. Bell, *J. Catal.*, **85** (1984) 143.
- [37] J.L. Falconer and R.J. Madix, *Surf. Sci.*, **48** (1975) 393.
- [38] M.A. Barteau and R.J. Madix, *Surf. Sci.*, **120** (1982) 262.
- [39] J.M. Vohs and M.A. Barteau, *Surface Science*, **176** (1986) 91.
- [40] J.M. Vohs and M.A. Barteau, *Surface Science*, **221** (1989) 590.
- [41] J.M. Vohs and M.A. Barteau, *Surface Science*, **201** (1988) 481.
- [42] J.M. Vohs and M.A. Barteau, *J. Phys. Chem.*, **91** (1987) 4766.
- [43] P.C. Stair, *J. Am. Chem. Soc.*, **104** (1982) 4044.
- [44] A. Zecchina, S. Coluccia, E. Guglielminotti and G. Ghiotti, *J. Phys. Chem.*, **75** (1971) 2790.
- [45] Harold S. Booth and Donald R. Martin, **Boron Trifluoride and Its Derivatives**, John Wiley and Sons, Inc., New York, 1949.
- [46] K.H. Schulz and D.F. Cox, *Phys. Rev. B*, **43** (1991) 1610.
- [47] D.F. Cox, T.B. Fryberger, and S. Semancik, *Phys. Rev. B*, **38** (1988) 2072.
- [48] D.F. Cox, T.B. Fryberger, and S. Semancik, *Surface Science*, **224** (1989) 121.
- [49] D.F. Cox and T.B. Fryberger, *Surface Science*, **227** (1990) 2105.
- [50] V.A. Gercher, *Ph.D. dissertation*, 1994.
- [51] V.A. Ralph and D.F. Cox, *Surface Science*, **306** (1994) 279.
- [52] D. Adler, *Solid State Physics*, **21** (1968) 83.
- [53] R.E. Newnham and Y.M. de Haan, *Zeitschrift für Kristallographie*, **27** (1962) 235.
- [54] V.E. Henrich and P.A. Cox, **The Surface Science of Metal Oxides** (Cambridge: Cambridge University Press, paperback edition, 1996).
- [55] Steven C. York, Mark W. Abee, and David F. Cox, *Surface Science*, **437** (1999) 386.
- [56] R.J. Lad and V.E. Henrich, *Surf. Sci.*, **193** (1988) 81.
- [57] S.C. York, *PhD dissertation*, 1999.
- [58] J.L. Loison, M. Robino and B. Schwab, *J. Cryst. Growth* **50** (1980) 816.
- [59] B. Thiel and R. Helbig, *J. Cryst. Growth*, **32** (1976) 259.
- [60] The ion gauge sensitivity for ammonia was taken as 1.3 per the Quadrex 200 Technical Manual, Inficon Leybold-Heraeus.
- [61] K.H. Schulz and D.F. Cox, *Surface Science*, **262** (1992) 318.